

Drain System Around the Underground Cavern

Isao MOTOJIMA*, Iichiro KONO** and Makoto NISHIGAKI**

(Received September 30, 1993)

SYNOPSIS

In recent years, construction or planning of large-scale underground structures, such as underground power plants, underground oil storage plants and nuclear power plants have been coming into consideration in Japan.

To construct such as large-scale underground structures, one of the most important problems is to make clear beforehand the behavior of groundwater around these structures and the other is to carry out proper countermeasure of groundwater, so that these structures can be constructed safely and maintained stability over a long time period.

This report describes the results of theoretical studies on the drain systems and at the same time, discusses the drain systems around the underground cavern for the practical underground power stations.

1. INTRODUCTION

In recent years, construction or planning of large-capacity pumped storage power stations, underground oil storage plants, underground nuclear power plants and other large-scale structures in the deep underground area have been coming into

* Central Research Institute of Electric Power Industry

** Department of Civil Engineerig

consideration in our country.

To construct such as large-scale underground structures, the most important problems is to make clear beforehand the behavior of groundwater in the bedrock as well as the bedrock condition and to carry out proper countermeasure of groundwater, so that these structures can be constructed safely and maintained stability over a long time period.

Many studies have so far been carried out to solve the groundwater hydraulic problems around the underground structures. These studies include the investigation on groundwater discharge to railway tunnels, road tunnels and other long tunnels⁽¹⁾, the investigation on the groundwater discharge⁽²⁾, the prediction for abnormal groundwater discharge during construction of tunnels in the Seikan Tunnel^{(3),(4)} and the effectiveness of drain systems for high pressure groundwater⁽⁵⁾. Moreover, with respect to the underground structures such as underground power plants, the studies include the consideration relation to unlined underground oil storage plants^{(6),(7)}, the consideration on hydraulic approaches to hydraulic and hydrologic problems in underground caverns⁽⁸⁾, etc.

In this paper, it is the purpose to examine the drain systems for decreasing the groundwater pressure around the caverns of underground power stations. And the Shin Takasegawa Power Station constructed by the Tokyo Electric Power Co., Inc. was investigated as the area around the underground cavern.

2. THEORETICAL STUDIES ON THE DRAIN SYSTEMS

2.1 Groundwater Level Around The Cavern

To examine the groundwater level around the underground cavern, a model as shown in Fig. 1 is assumed under the following point. When a cavern is excavated in the bedrock including groundwater, the groundwater is discharged in the cavern. If a lot of amount of water is discharged, it not only

constitutes an obstacle to cavern excavation but also exerts an adverse effect on the stability of the cavern. But, this water discharge induces a drain effect, the groundwater level around the cavern become decrease .

Meanwhile, due to its excavation, relaxed phenomena including the opening and breaking of joints is developed in the bedrock around the cavern, thereby a relaxed zone with high permeability is forming around the cavern⁽⁹⁾. This phenomena serves to accelerate the drain effect around the cavern.

Also, for excavation such as a large cavern, lock bolts and shotcrete are applied so as to maintain stability to the cavern and to protect the cavern wall surface. The permeability of this shotcreted zone is considerably smaller than the relaxed zone of bedrock. Thus it is suppressed the generation of water discharge in the cavern.

By applying the Dupuit-Forchheimer's hypothesis to each layer shown in Fig. 1, the groundwater level at each point is obtained as follows :

$$h_3^2 = H^2 - 2K_{01} (\sqrt{K_0^2 + H^2} - K_0) \dots\dots\dots (1)$$

$$h_2^2 = H^2 - 2(K_{01} + K_2) (\sqrt{K_0^2 + H^2} - K_0) \dots\dots\dots (2)$$

$$h_1^2 = H^2 - 2K_0 (\sqrt{K_0^2 + H^2} - K_0) \dots\dots\dots (3)$$

$$h_{00}^2 = H^2 - 2K_{01} l_{01} (\sqrt{K_0^2 + H^2} - K_0) \dots\dots\dots (4)$$

where

$$K_0 = \frac{l}{K} K_3 \qquad K = \frac{l}{\frac{l_1}{K_1} + \frac{l_2}{K_2} + \frac{l_3}{K_3}}$$

$$K_{01} = \frac{l_1}{K_1} K_3 \qquad l = l_1 + l_2 + l_3$$

$$K_{02} = \frac{l_2}{K_2} K_3 \qquad l_{01} = \frac{l_0}{l_1}$$

Where, the point at the distance l from the cavern is assumed to be $X = 0$, and this point is the boundary of influence circle where groundwater level decreasing by drain effect of the

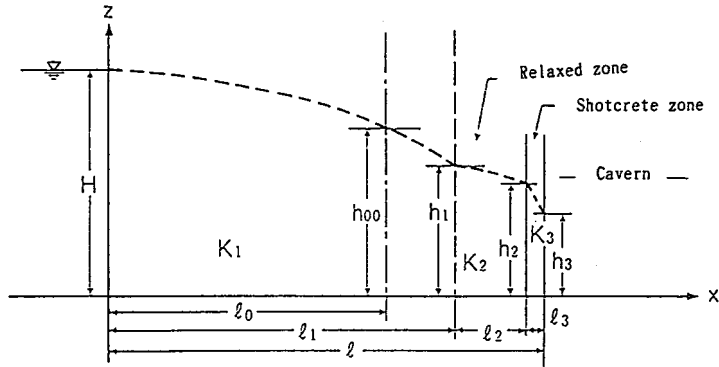


Fig.1 Analysis model of the groundwater level.

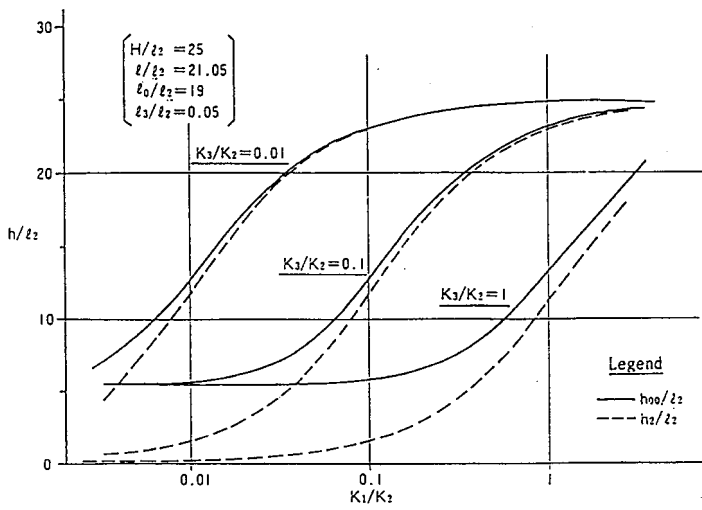


Fig.2 Effect of k_1/K_2 for the groundwater level.

cavern. Permeability in the bedrock, relaxed zone and shotcreted zone are expressed as k_1 , k_2 and K_3 , respectively. Thickness of each zone are expressed as l_1 , $l_1 + l_2$, l_3 , groundwater levels in the boundary of each zone and the groundwater level at the discharge point into the cavern are expressed as h_1 , h_2 and h_3 , respectively. Moreover, the groundwater level at any point ($X = l_0$) in the bedrock is expressed as h_{00} .

The relationships between the groundwater level h , h and the permeability K_1 , K_2 and K_3 in each zone which are calculated by using a equation (1)~(4) are shown in Fig. 2. In case of the permeability ratio of bedrock and relaxed zone is $K_1/K_2 = 0.1$, the groundwater level h_2 in the boundary between the relaxed zone and the shotcreted zone decreases to 6 % of the natural groundwater level H , as well as when the permeability ratio of shotcreted zone to relaxed zone is equal with $K_3/K_2 = 1$. With $K_3/K_2 = 0.01$, however, the decreasing the groundwater level is 92 %, showing little decrease. Next, in case of $K_1/K_2 = 0.01$, the groundwater level h decreases to 0.08 % with $K_3/K_2 = 1$. With $K_3/K_2 = 0.01$, however, the decreasing the groundwater level is 46.8 %. Similar relationships are also found with groundwater level h_{00} behind the relaxed zone.

The groundwater level around the cavern is dependent on the permeability in each zone, particularly on the permeability in relaxed zone (high-permeable zone) due to excavation of cavern and is decreases as the permeability in relaxed zone becomes larger. Also, this groundwater level is decreases as the permeability in shotcreted zone becomes larger. However, the permeability of shotcreted zone is generally far smaller than that of the relaxed zone, thereby high groundwater level will remain in relaxed zone behind shotcreted zone.

2.2 Decreasing The Groundwater Pressure By Vertical Drain Boreholes

The existence of such a high groundwater level, namely pressure, behind shotcreted zone is not desirable for the stability of the cavern. To decrease this high groundwater pressure, therefore, the drain boreholes with diameter $2r_0$ on

$x = l_0$ at borehole spacing d_0 were arranged as shown in Fig. 3. Such a problem can be solved by the Image Method in which sinks are arranged at point of $Y = nd$ on $X = l_0$ and sources are arranged at point of $Y = nd$ on $X = -l_0$, infinitely in respective cases .

The complex potential ζ in this case can be expressed as follows :

$$\begin{aligned} \zeta &= M \sum_{n=-\infty}^{\infty} \ln \{ z - (nd_0 + il_0) \} - M \sum_{n=-\infty}^{\infty} \ln \{ z - (nd_0 - il_0) \} \\ &= M \ln (z - il_0) - M \ln (z + il_0) \\ &\quad + M \ln \prod_{n=1}^{\infty} \left\{ \left(\frac{z - il_0}{nd_0} \right)^2 - 1 \right\} - M \ln \prod_{n=1}^{\infty} \left\{ \left(\frac{z + il_0}{nd_0} \right)^2 - 1 \right\} \\ &= M \ln \frac{\sin \frac{\pi}{d_0} (z - il_0)}{\sin \frac{\pi}{d_0} (z + il_0)} \\ &= M \ln \frac{\sin \frac{\pi}{d_0} \{ y + i(x - l_0) \}}{\sin \frac{\pi}{d_0} \{ y + i(x + l_0) \}} \dots\dots\dots (5) \end{aligned}$$

In equation (5),

$$M = \frac{q_0}{2\pi}$$

$(0, Y)$: Potential of the line source on $KH_0(0, Y)$,

$-q_0$: The discharge flow rate per unit length of one vertical drain borehole.

Then, the potential ϕ becomes as follows :

$$\begin{aligned} \phi &= \frac{q_0}{2\pi} \ln \left| \frac{\sin \frac{\pi}{d_0} \{ y + i(x - l_0) \}}{\sin \frac{\pi}{d_0} \{ y + i(x + l_0) \}} \right| + KH_0 \\ &= \frac{q_0}{2\pi} \ln \frac{\cosh \frac{2\pi}{d_0} (x - l_0) - \cos \frac{2\pi}{d_0} (y)}{\cosh \frac{2\pi}{d_0} (x + l_0) - \cos \frac{2\pi}{d_0} (y)} + KH_0 \end{aligned}$$

Here, the potential of the vertical drain borehole is expressed as $\phi(\ell_0 - r, 0) = Khwo$. Then,

$$h_{wo} = \frac{q_0}{2\pi K} \ln \frac{\cosh \frac{2\pi}{d_0}(r_0) - 1}{\cosh \frac{2\pi}{d_0}(2\ell_0 - r_0) - 1} + H_0$$

$$h_{wo} = \frac{q_0}{2\pi K} \ln \frac{\cosh \frac{2\pi}{d_0}(r_0) - 1}{\cosh \frac{4\pi}{d_0}(\ell_0) - 1} + H_0$$

($\ell_0 \gg r_0$)

$$= \frac{q_0}{2\pi K} \ln \frac{\sinh \frac{\pi}{d_0}(r_0)}{\sinh \frac{2\pi}{d_0}(\ell_0)} + H_0$$

$$\therefore -q_0 = \frac{\pi K(H_0 - h_{wo})}{\ln \frac{\sinh \frac{\pi}{d_0} \ell_0}{\sinh \frac{2\pi}{d_0} r_0}}$$

Thus, the groundwater head h on $X = \ell_0$ becomes as follows :

$$h = H_0 - \frac{H_0 - h_{wo}}{2 \ln \frac{\sinh \frac{\pi}{d_0} r_0}{\sinh \frac{2\pi}{d_0} \ell_0}} \ln \frac{1 - \cos \frac{2\pi}{d_0} y}{\cosh \frac{2\pi}{d_0}(2\ell_0) - \cos \frac{2\pi}{d_0} y} \dots \dots \dots (6)$$

From equation (6), the groundwater head h_0 at an intermediate point ($X = \ell_0, y = 0.5 nd_0$) between drain boreholes becomes as expressed by the following equation :

$$h_0 = H_0 - \frac{H_0 - h_{wo}}{2 \ln \frac{\sinh \frac{2\pi}{d_0} \ell_0}{\sinh \frac{\pi}{d_0} r_0}} \ln \frac{\cosh \frac{2\pi}{d_0}(2\ell_0) + 1}{2} \dots \dots \dots (7)$$

Figs. 4~6 shows the relationships between the groundwater head h_0 at an intermediate point between drain boreholes and the borehole spacing d_0 , the natural groundwater head H_0 , and the borehole diameter $2r_0$ on the basis of equation (7).

The groundwater head h_0 increases as the borehole spacing d_0

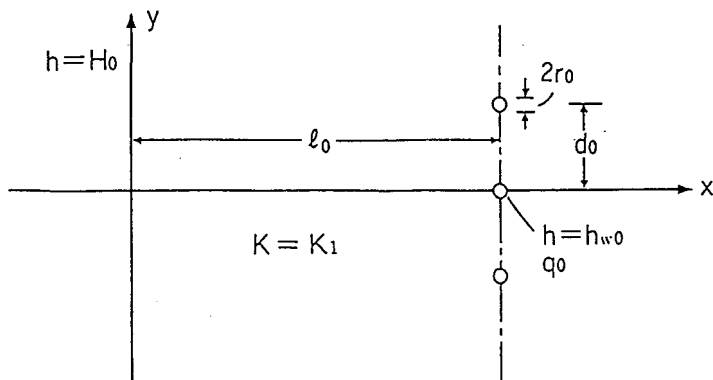


Fig.3 Analysis model of the vertical drain boreholes.

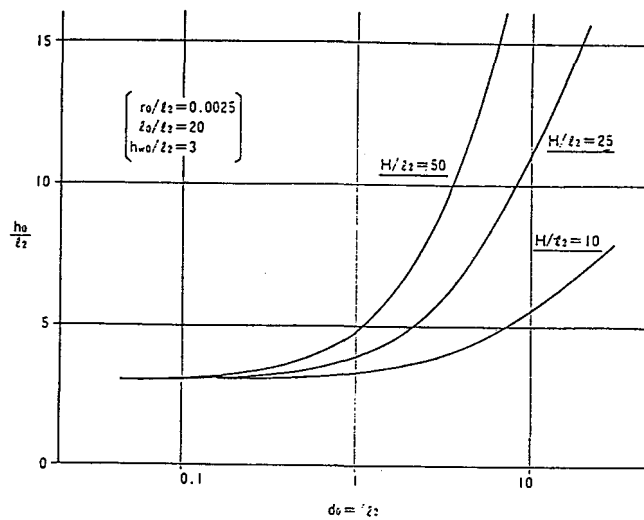


Fig.4 Effect of d_0 for the groundwater head at the intermediate point between the vertical drain boreholes.

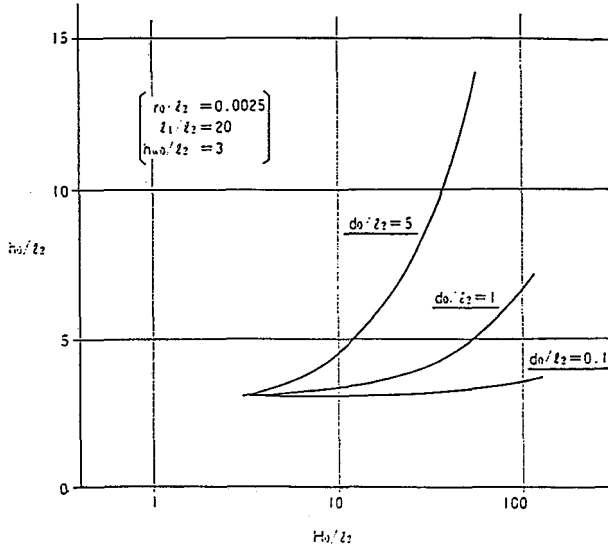


Fig.5 Effect of H_0 for the groundwater head at the intermediate point between the vertical drain boreholes.

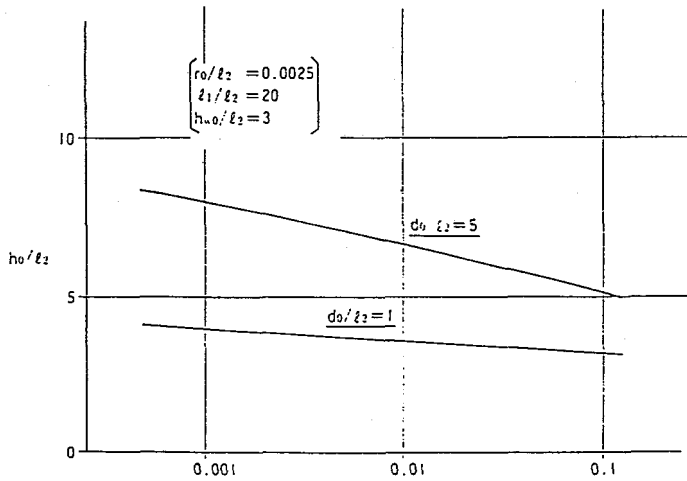


Fig.6 Effect of r_0 for the groundwater head at the intermediate point between the vertical drain boreholes.

becomes larger. Similar relationships are also found with the natural groundwater head H_0 . While, the groundwater head h_0 decreases as the borehole diameter $2r_0$ becomes larger. In the case of $r_0/l_2 < 0.01$, it decreases rapidly but this decrease is slight at $r_0/l_2 > 0.01$.

When the width of the relaxed zone is assumed to be $l_2 = 10\text{m}$ approximately, effect of the drain boreholes are shown a linear increase as the borehole spacing d_0 becomes larger. But, at $r_0 > 100\text{ mm}$, its effect is small as the borehole diameter becomes larger.

Drain borehole effect by reducing the borehole spacing d_0 is larger than by increasing borehole diameter $2r_0$.

2.3 Groundwater Level At The Behind Of Shotcreted Zone

When the vertical drain boreholes are arranged as described in the preceding subsection, the groundwater head h_2 at the behind of shotcreted zone is calculated using equation (2) with condition that the groundwater head h_{00} at $X = l_2$ is assumed to be equal to the groundwater head h_0 at an intermediate point between the drain boreholes arranged on this line.

Its results are shown in Fig. 7. When the permeability of shotcreted zone K_3 becomes smaller as compared with the permeability of the relaxed zone K_2 , the groundwater head h_2 is closer to groundwater head on $X = l_2$ on which the vertical drain boreholes are arranged. This tendency becomes larger as the ratio of bedrock permeability K_1 to relaxed zone permeability K_2 increases. Generally, the permeability of shotcreted zone is far smaller than that of the relaxed zone, so the groundwater head h_2 will become almost equal to the groundwater head on $X = l_0$.

The discharge flow rate Q into the cavern can be expressed by the following equation :

$$Q = K_3 (\sqrt{K_0^2 + H^2} - H^2) \dots\dots\dots (8)$$

In Fig. 8, the discharge flow rate Q into the cavern is calculated from equation (8).

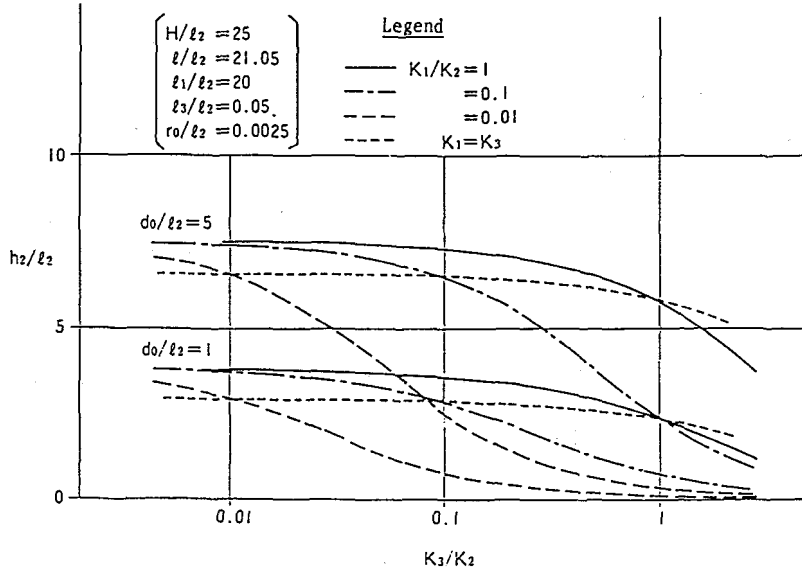


Fig.7 Relationship between h_2 / Q_2 and $k_1 / k_2 , k_3 / k_2$.

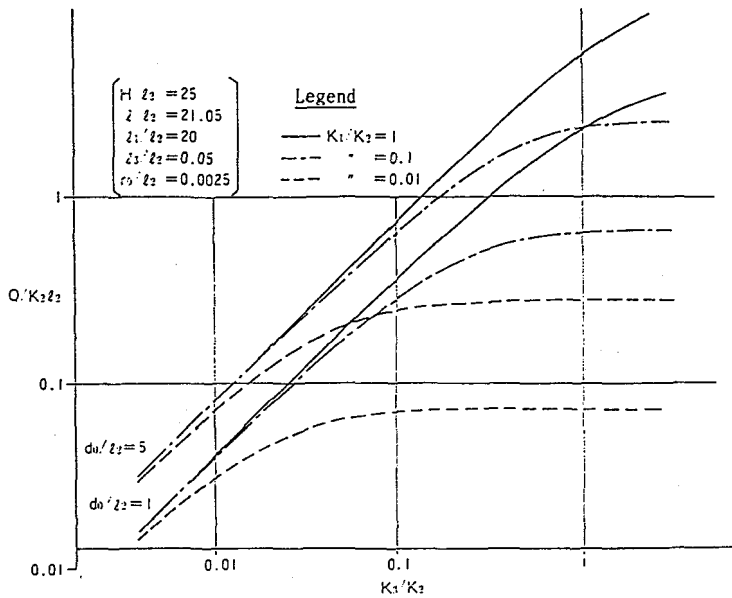


Fig.8 Discharge flow rate into the cavern.

2.4 Decreasing The Groundwater Pressure By Horizontal Drain Boreholes

To decrease the groundwater pressure remaining the behind of shotcreted zone, the horizontal drain boreholes are arranged in the base of cavern wall as shown in Fig. 9. The discharge flow rate to the boreholes can be solved by the Image Method in which sinks are arranged at a point of $X = md$ on $y = (4n+1)T$ and sources at a point of $X = md$ on $y = (4n-1)T$, infinitely in respective cases.

The complex potential ζ in this case can be expressed as follows :

$$\begin{aligned} \zeta &= M \sum_{n=-\infty}^{\infty} \ln(z - \{md + i(4n+1)T\}) \\ &\quad - M \sum_{n=-\infty}^{\infty} \ln(z - \{md + i(4n-1)T\}) \\ &= M \sum_{n=-\infty}^{\infty} \ln(z - i(4n+1)T) \\ &\quad - M \sum_{n=-\infty}^{\infty} \ln(z - i(4n-1)T) \\ &\quad + M \sum_{n=-\infty}^{\infty} \ln \frac{\prod_{m=1}^{\infty} \left(1 - \frac{\{z - i(4n+1)T\}^2}{(md)^2} \right)}{\prod_{m=1}^{\infty} \left(1 - \frac{\{z - i(4n-1)T\}^2}{(md)^2} \right)} \\ &= M \sum_{n=-\infty}^{\infty} \ln \frac{\sin \frac{\pi}{d} \{z - i(4n+1)T\}}{\sin \frac{\pi}{d} \{z - i(4n-1)T\}} \dots\dots\dots (9) \end{aligned}$$

In equation (9),

$$M = \frac{q}{\pi}$$

$$(x, 0) = KT,$$

-q : discharge flow rate per unit length of one horizontal drain borehole.

Then, the potential ϕ becomes as follows :

$$\phi = \frac{-q}{\pi} \sum_{n=-\infty}^{\infty} \ell_n \frac{|\sin \frac{\pi}{\ell} \{z - i(4n+1)T\}|}{|\sin \frac{\pi}{\ell} \{z - i(4n-1)T\}|} + KT$$

Here, the potential of the horizontal drain borehole is expressed as $\phi(0, T-r) = Kh_d$, then

$$\begin{aligned} h_d &= \frac{-q}{2\pi K} \ell_n \frac{\cosh \frac{2\pi}{\ell} (r) - 1}{\cosh \frac{2\pi}{\ell} (2T-r) - 1} \\ &+ \sum_{n=1}^{\infty} \ell_n \frac{(\cosh \frac{2\pi}{\ell} \{-r\} - 4nT)(\cosh \frac{2\pi}{\ell} \{-r\} + 4nT - 1)}{(\cosh \frac{2\pi}{\ell} (2T-r) - 4nT - 1)(\cosh \frac{2\pi}{\ell} (2T-r + 4nT) - 1)} \ell_n + T \\ &= \frac{-q}{\pi K} \ell_n \frac{\sinh \frac{\pi}{\ell} (r)}{\sinh \frac{\pi}{\ell} (2T-r)} \\ &+ \sum_{n=1}^{\infty} \ell_n \frac{[1 - \coth^2 \frac{\pi}{\ell} (-r) \tanh^2 \frac{\pi}{\ell} (4nT)] \sinh^2 \frac{\pi}{\ell} (r)}{[1 - \coth^2 \frac{\pi}{\ell} (2T-r) \tanh^2 \frac{\pi}{\ell} (4nT)] \sinh^2 \frac{\pi}{\ell} (2T-r)} \ell_n + T \end{aligned}$$

Thus, the discharge flow rate q can be expressed by the following equation :

$$\begin{aligned} -q &= \frac{\pi K (h - h_d)}{\ell_n \frac{\sinh \frac{\pi}{\ell} (r)}{\sinh \frac{\pi}{\ell} (2T-r)} + \sum_{n=1}^{\infty} \ell_n \frac{[1 - \coth^2 \frac{\pi}{\ell} (-r) \tanh^2 \frac{\pi}{\ell} (4nT)] \sinh^2 \frac{\pi}{\ell} (r)}{[1 - \coth^2 \frac{\pi}{\ell} (2T) \tanh^2 \frac{\pi}{\ell} (4nT)] \sinh^2 \frac{\pi}{\ell} (2T)}} \\ &= \frac{\pi K (h - h_d)}{\ell_n \frac{\sinh \frac{\pi}{\ell} (r)}{\sinh \frac{\pi}{\ell} (2T)} + \sum_{n=1}^{\infty} \ell_n \frac{[1 - \coth^2 \frac{\pi}{\ell} (-r) \tanh^2 \frac{\pi}{\ell} (4nT)] \sinh^2 \frac{\pi}{\ell} (r)}{[1 - \coth^2 \frac{\pi}{\ell} (2T) \tanh^2 \frac{\pi}{\ell} (4nT)] \sinh^2 \frac{\pi}{\ell} (2T)}} \\ &\quad (2T - r \doteq 2T) \\ &\dots\dots\dots (10) \end{aligned}$$

When the length of the horizontal drain borehole is ℓ_2 ,

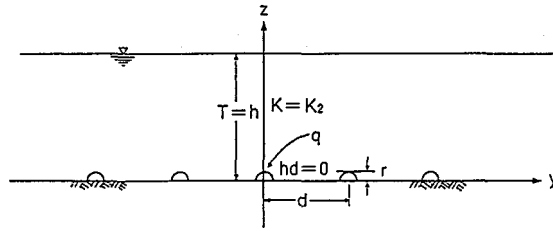


Fig.9 Analysis model of the horizontal drain boreholes.

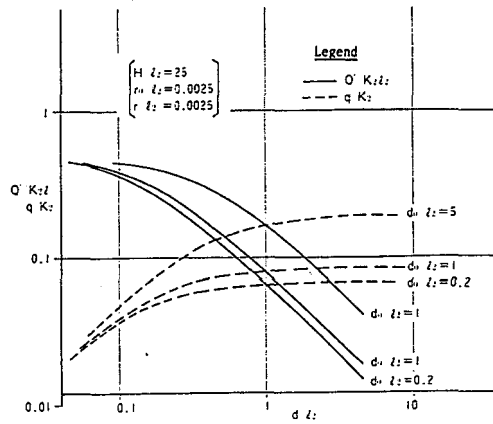


Fig.10 Effect of d for discharge flow rate into the horizontal drain boreholes.

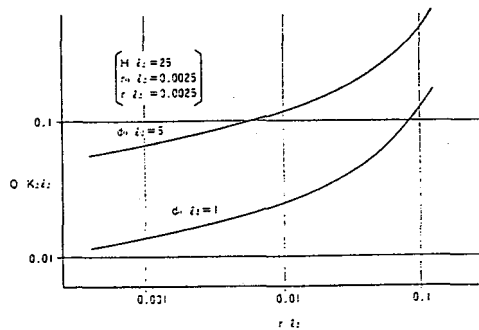


Fig.11 Effect of r for discharge flow rate into the horizontal drain boreholes.

then the discharge flow rate Q' per unit length of cavern wall can be obtained as follows :

$$Q' = q l_2 / d \quad \dots\dots\dots(11)$$

Figs. 10 and 11 shows the relationships between the discharge flow rate q , Q' and the boreholes spacing d , the borehole diameter $2r$ on the basis of equations (10) and (11). The discharge flow rate Q' is almost inversely to the borehole spacing d , especially, it increases rapidly as borehole spacing becomes decreasing at $d/l_2 > 0.1$. While, this discharge flow rate Q' is in proportion to borehole diameter $2r$.

When the width of the relaxed zone is assumed to be $l_2 = 10$ m approximately, effect of horizontal drain boreholes by reducing its borehole spacing d is larger rather than by increasing the diameter of boreholes $2r$ at $r < 100$ mm.

3. STUDY ON THE DRAIN SYSTEM AT THE CAVERN FOR SHIN TAKASEGAWA POWER STATION

The theoretical study considered in the preceding chapter is discussed on the drain system using the area around the cavern for the Shin Takasegawa Underground Power Station constructed by Tokyo Electric Power Co., Inc. as a model.

The Shin Takasegawa Power Station, located in the midstream of the Takase River in Nagano Prefecture, is a pumped storage type underground power station with maximum output power of 1,280 MW. The cavern for this power station is a large underground cavern measuring 54.5 m high, 27 m wide and 165 m long. The generator room floor level(EL 1,003 m) is 46 m below the high water level(EL 1,049 m) in the lower reservoir and is located relatively close to the ground surface. Moreover, the Shishinokuchi fault presents in the vicinity, in which a high groundwater pressure exists. For these reason, the water discharge to the cavern was feared to occur.

3.1 Geological Features And Permeability Of Bedrock Around

The Cavern For The Underground Power Station

(1) Outline of geological features

The geological map of this site is shown in Fig. 12(Hori, 1980). The cavern for the underground power station was selected in the area where granite, diorite and mottled fine-grained diorite are distributed.

The results of the laboratory tests on boring cores are shown in Table 1⁽¹⁰⁾. Moreover, the joint frequency is about 4 joints/m, and their predominant direction is shown in Fig. 13⁽¹¹⁾.

The longitudinal axis of the cavern is located in the N 80° W direction.

(2) Permeability of bedrock

Fig. 14 shows the relationship between the permeability and depth of bedrock on the basis of Lugeon test results. The permeability of bedrock is as high as 30 Lugeons or more in about 20 m close to the ground surface, several Lugeons in the deeper zone than 50m, and 1 Lugeon or less around the cavern.

Fig. 15 shows the results of Lugeon tests in 12 boreholes made around the cavern. On the basis of this figure, average permeability are summarized in Table 2. In bedrock around the cavern, there are some parts that show 5 Lugeons or more. As a whole, however, the permeability is 1 Lugeon or less, and the average permeability is as small as 0.38 Lugeon(standard deviation : 0.29 Lugeon).

Next, the permeability changes in bedrock mass due to excavation of the cavern are shown in Fig. 16⁽⁹⁾. The permeability of the bedrock around the cavern changed several 100 times in the vicinity of the cavern(around 10 m) due to its excavation, reaching 30 55 Lugeons(before excavation; 0.03 0.1 Lugeon). At the zone of approximately 20m from the cavern wall, the average permeability changed to several 10 times.

3.2 Groundwater Around The Cavern

The change of groundwater level around the cavern large from season to season. The results of measurements on the groundwater discharge in the penstock shaft are shown in Fin. 17.

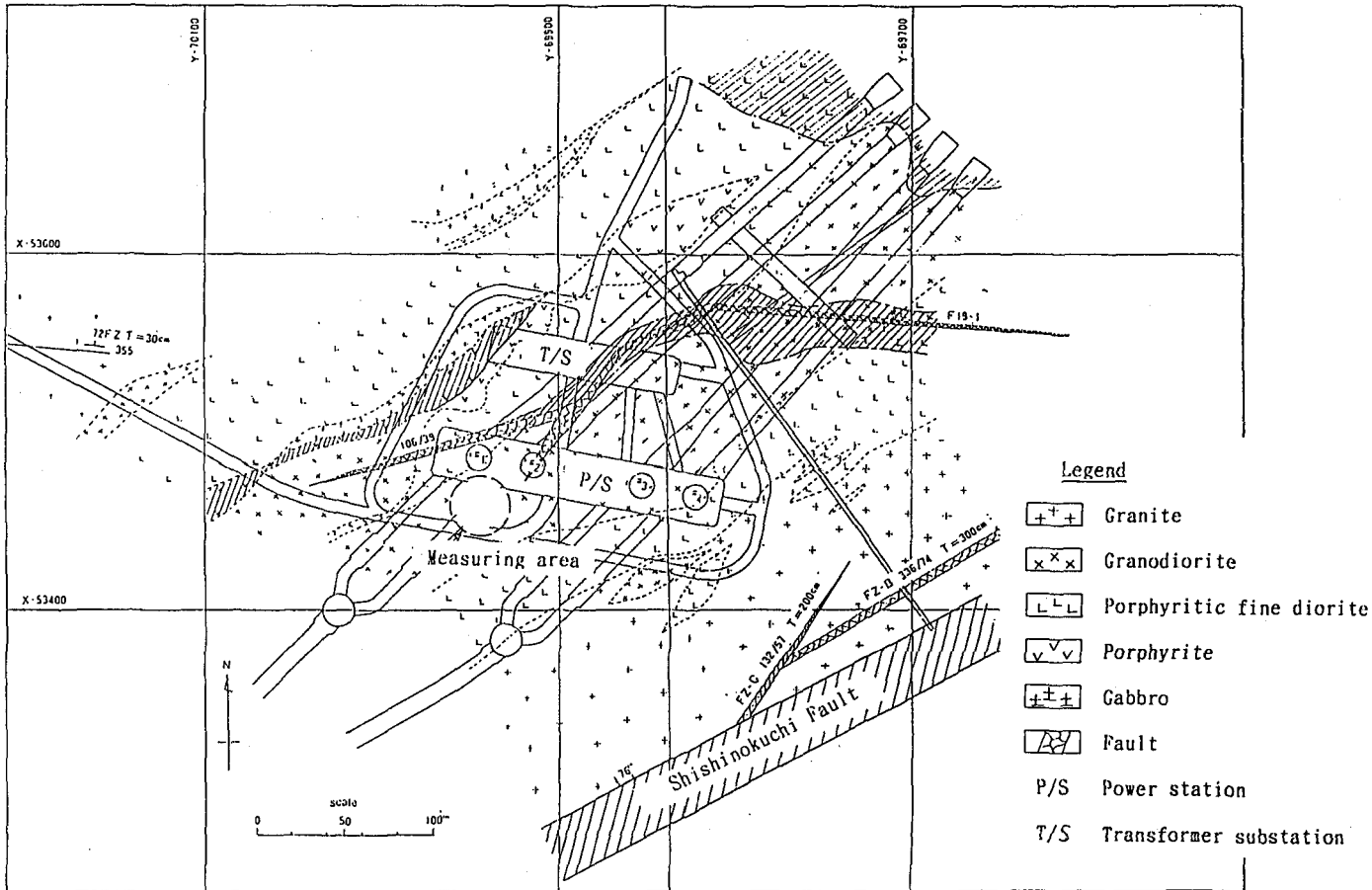


Fig.12 Geological map at Shintakasegawa power station site.

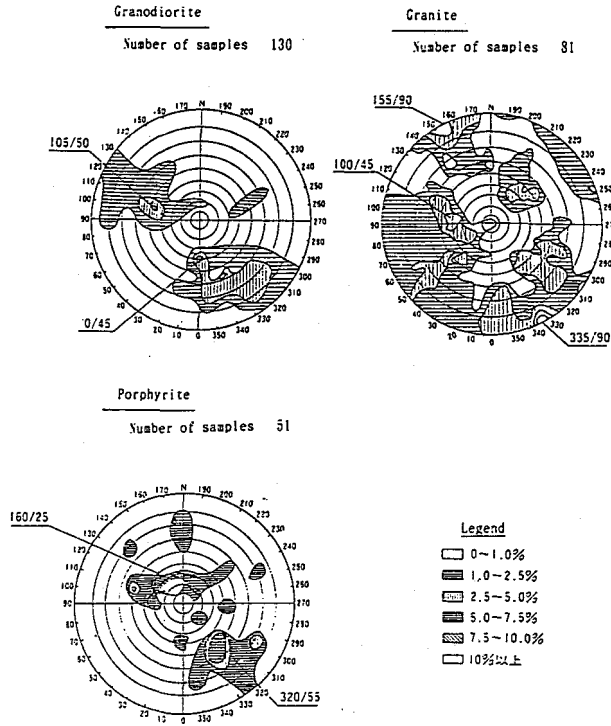


Fig.13 Ulf's net of joints in rock mass around the power station.

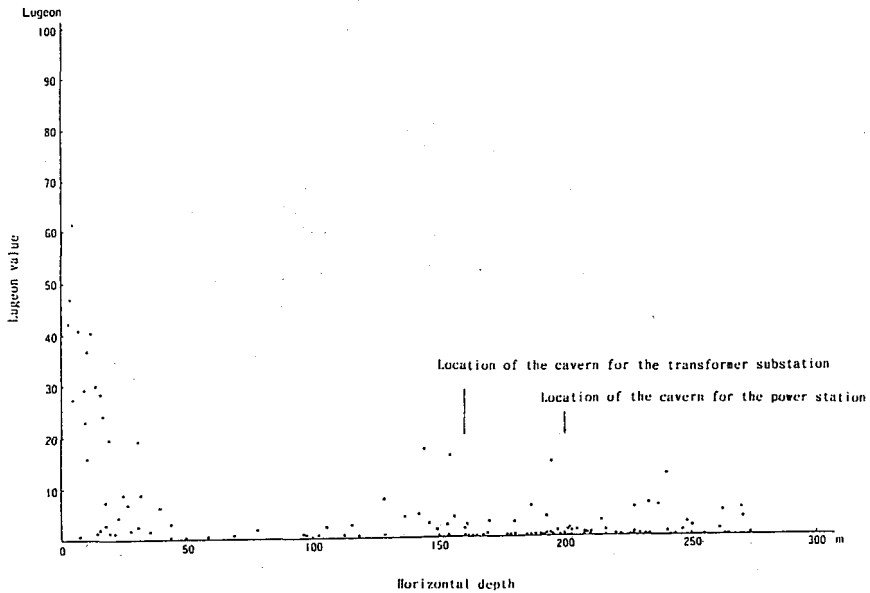


Fig.14 Relationship between the Lugeon value and Horizontal depth.

Table 1 Strength of rocks for Granodiorite (Results of rock tests).

	Density g/cm	Effective porosity %	Compression strength Kg/cm	Tensile strength Kg/cm	Shearing strength Kg/cm
Dry	2.620	1.7	2.167	62.8	456
Wet	2.636	1.7	1.911	61.1	409

Table 2 Permeability of rock mass for Granodiorite (Results of Lugeon test).

	Numbers	Maximum Lugeon	Minimum Lugeon	Mean Lugeon	standard deviation Lugeon
B	15	0.78	0.03	0.34	0.21
C	37	6.38	0.06	0.68	1.35
Total	76	6.38	0.03	0.38	0.29

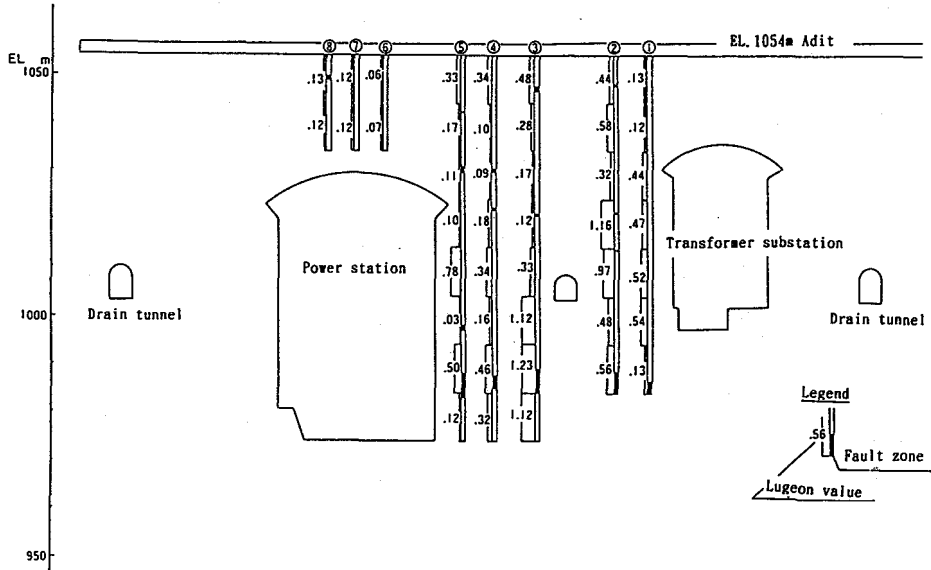


Fig.15-1 Distribution of permeability in rock mass around the power station.

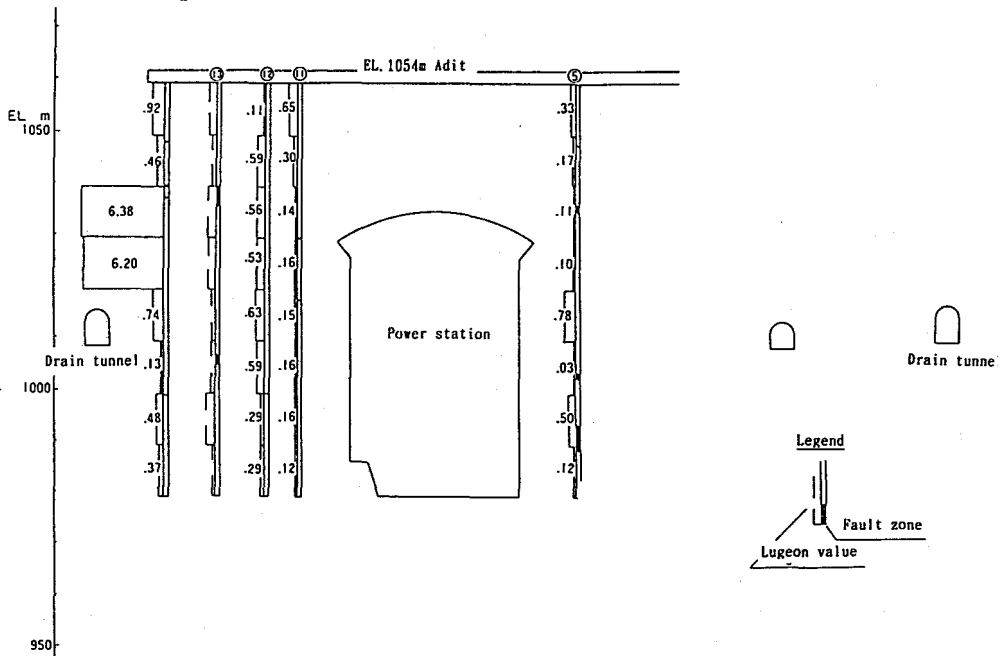


Fig.15-2 Distribution of permeability in rock mass around the power station.

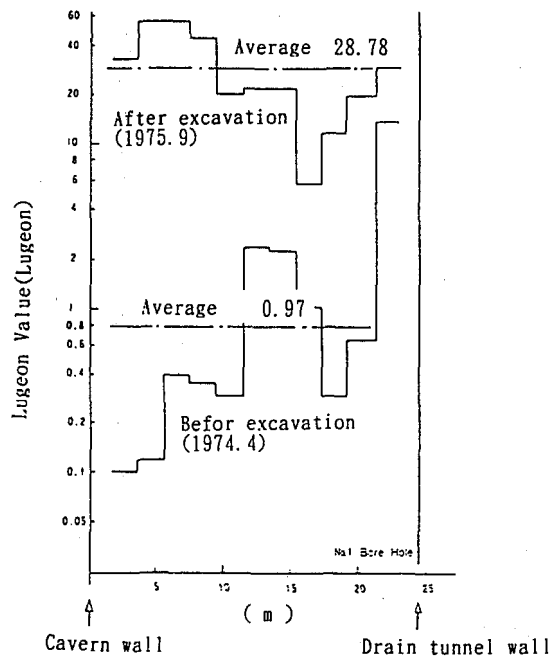


Fig.16-1 Permeability change of rock mass due to underground excavation.

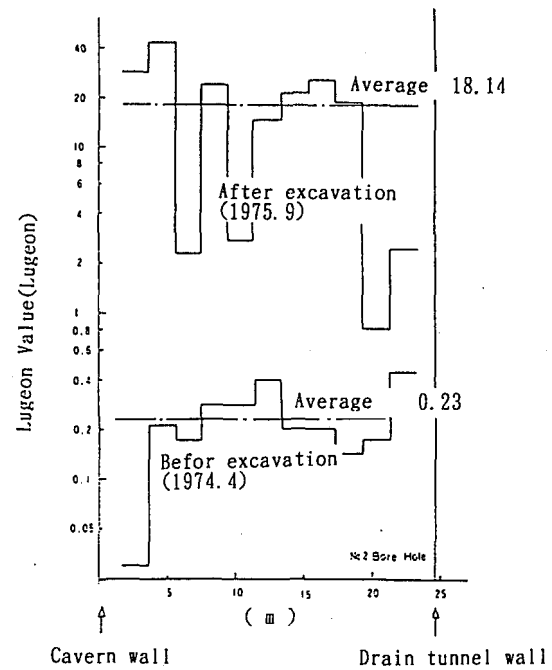


Fig.16-2 Permeability change of rock mass due to underground excavation.

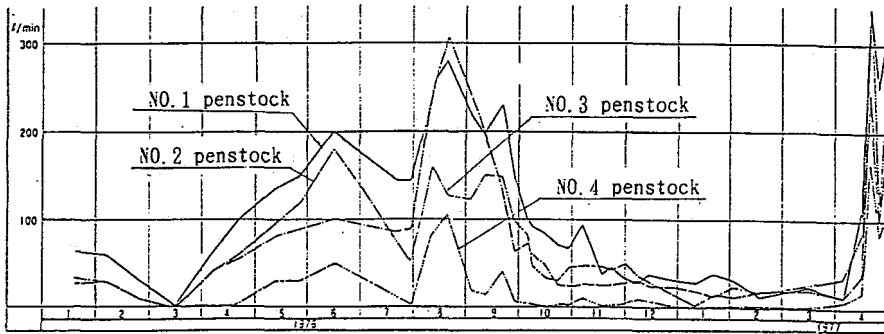


Fig.17 Discharge flow rate into the penstock.

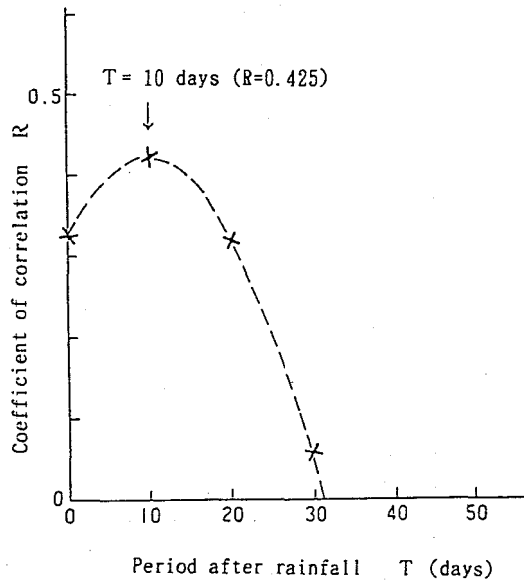


Fig.18 Correlation between of the groundwater discharge flow rate and period after rainfall

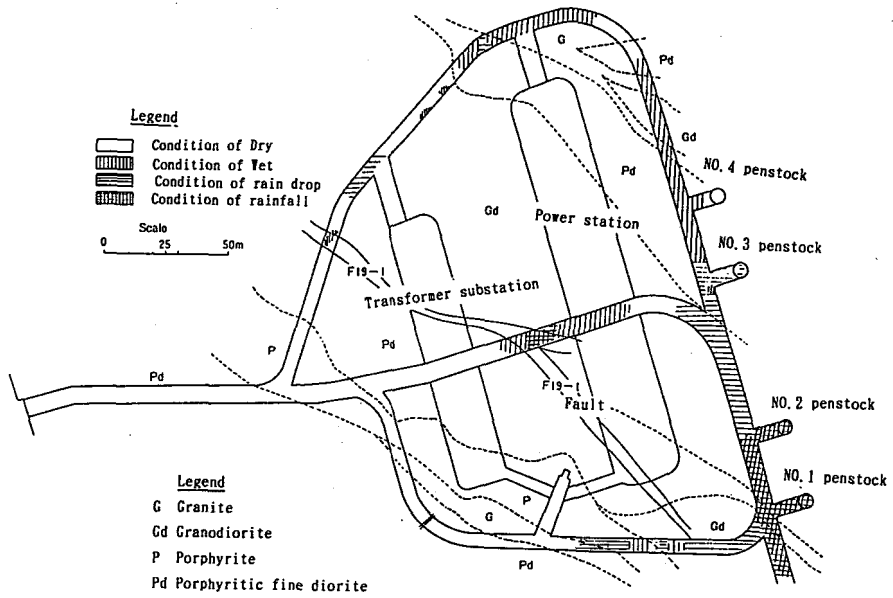


Fig.19-1 Condition of dry or wet in drain tunnel(1973.3.18).

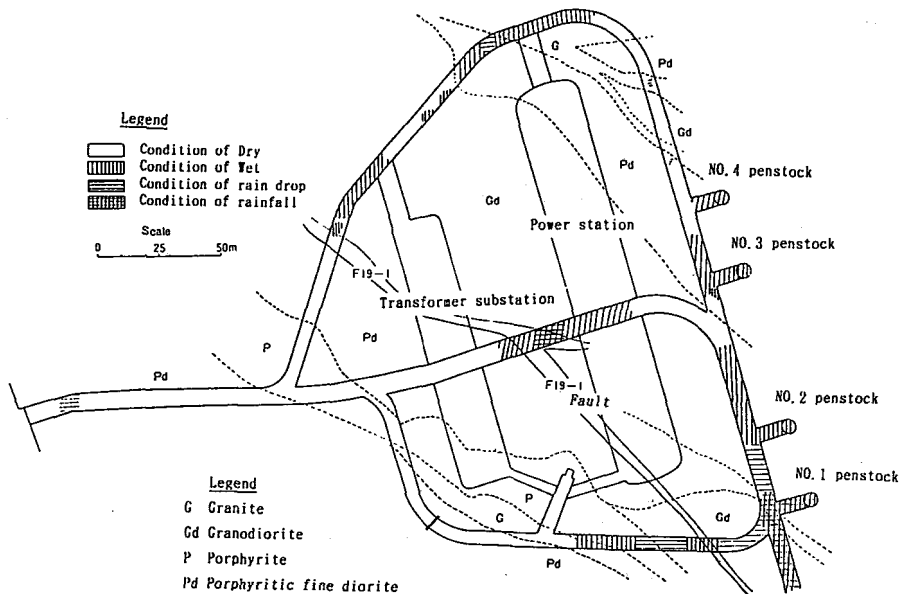


Fig.19-2 Condition of dry or wet in drain tunnel(1973.4.8).

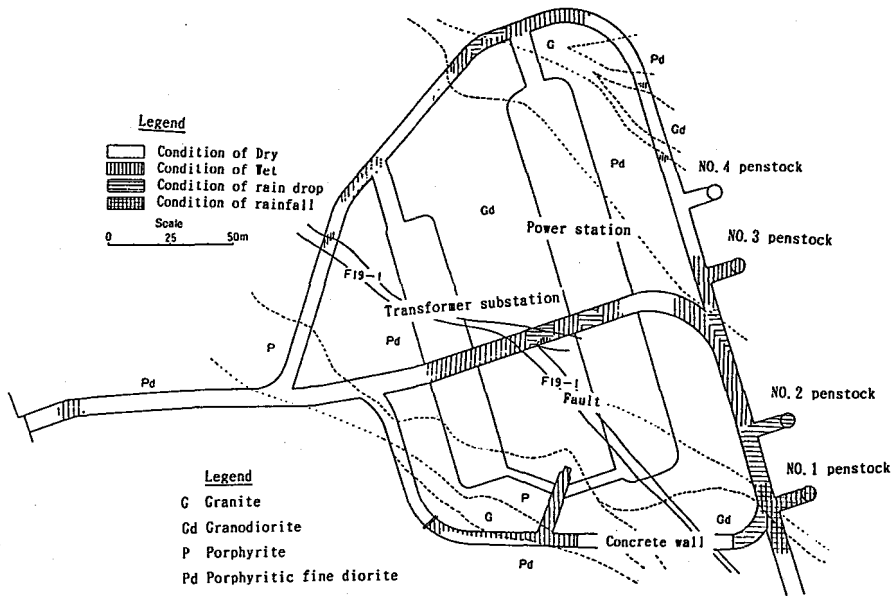


Fig.19-3 Condition of dry or wet in drain tunnel(1973.6.17).

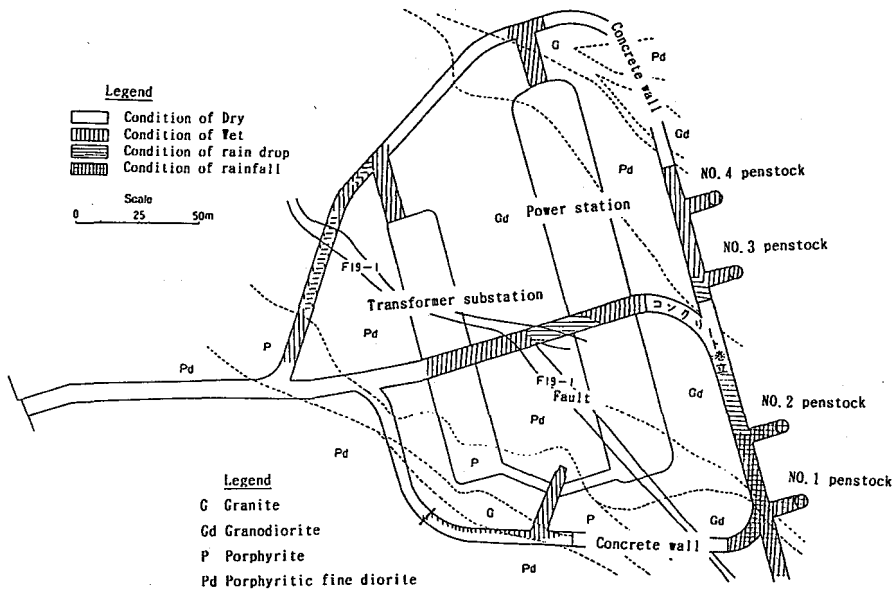


Fig.19-4 Condition of dry or wet in drain tunnel(1973.10.8).

The groundwater discharge became peak values in June for the snow thawing season and the rainy season overlap and in August to September which are thunderstorm and typhoon seasons, and reaches the lowest in winter for the snow season, thus indicating a typical mountain-type change.

The discharge flow rate shows a considerable correlation with the amount of rainfall as shown in Fig. 18. The coefficient of correlation between the discharge flow rate and the amount of rainfall indicates a peak in daily variation $\Delta T = 10$ days from a rainy day. This possibly means that the groundwater discharge is affected in 10 days after rainfall.

The results of observations conducted in the almost whole year on wet or dry and the groundwater discharge conditions in the drain tunnel around the cavern are shown in Fig. 19. The figure shows seasonal fluctuations in this groundwater discharge conditions and at the same time indicates that the groundwater discharge is concentrated in Nos. 1 and 2 penstock in the whole year.

Meanwhile, The Shishinokuchi fault which shows in Fig. 12 is a large-scale fault with a width of 30 m. Because of the existence of high-pressure groundwater (pressure : 10 kgf/cm² or more) at the survey time, it was difficult to excavate not only the adit but also the horizontal boreholes, and in the areas where the fault section was excavated, the discharge flow rate of 100 ~ 300 l/min was confirmed.

3.3 Study On The Drain System

To examine the drain system around the cavern for power station, in groundwater pressure, taking into consideration the geologic features, permeability, groundwater conditions, etc., each constants as shown in Figs. 1, 3 and 9 were established as follows :

(1) Permeability K_1 , K_2 and K_3 in each zone, based on Lugeon tests are set as follows :

$$K_1 = 0.5 \quad \text{Lugeon}$$

$$K_2 = 50 \quad \text{Lugeon}$$

$$K_3 = 1 \sim 0.5 \text{ Lugeon}$$

(2) The natural groundwater head H and the point at distance

(point of influence circle decreasing groundwater level) from the cavern is estimated as follows, taking into consideration the condition of the groundwater discharge to the investigated adits and penstock, the existence of the Shishinokuchi fault, etc:

$$l = 210.5 \text{ m}$$

$$H = 250 \text{ m}$$

(3) The thickness l_2 of the relaxed zone around the cavern is set as follows based on the measured results concerning changes in permeability around the cavern:

$$l_2 = 10 \text{ m}$$

(4) The thickness l_3 of shotcreted zone on the cavern wall is set as follows:

$$l_3 = 0.5 \text{ m}$$

(5) Vertical drain boreholes is assumed to make holes upward from the drain tunnel (EL 1003 m) around the cavern.

$$l_0 = 190 \text{ m}$$

$$h_{w0} = 30 \text{ m (EL 1010 m)}$$

(6) Horizontal drain boreholes is assumed to make holes in the base of the cavern wall, and vertical and horizontal borehole diameters $2r_0$, $2r$ are set as follows:

$$2r_0 = 2r = 50 \text{ mm}$$

(7) The elevation of impervious bedrock is assumed to be the bottom of the cavern (EL 980 m).

When drain boreholes are not arranged, groundwater levels at each position as shows Fig. 1 are calculated using equations (1) ~ (4). The results thus obtained are as follows:

$$h_{00} = 130.1 \text{ m (EL 1110.1 m)}$$

$$h_1 = 120.5 \text{ m (EL 1100.5 m)}$$

$$h_2 = 120.4 \text{ m (EL 1100.4 m)}$$

The groundwater levels at each position become much higher than the arch crown elevation (EL 1028.5 m) of the cavern.

Next, the vertical drain boreholes are arranged on the drain tunnel around the cavern, and the relationship between the groundwater head h_0 at an intermediate point between vertical drain boreholes and the borehole spacing d_0 is obtained using equation (7) as shown in Fig. 20. Also, the relationship between this groundwater head h_0 and the groundwater head h_2 at

the behind of shotcreted zone is obtained by equation (2) as shown in Fig. 21. When the vertical drain borehole spacing d_0 is smaller than 25.0 m, groundwater head h_2 becomes lower than the arch crown elevation of the cavern, however, a high groundwater head remains at the behind of shotcreted zone.

Then, horizontal drain boreholes are arranged in the base of the cavern wall, and the relationship between the horizontal drain borehole spacing d and the discharge flow rate Q'/d per unit width of cavern base into borehole (length : 10 m) is obtained using equations (10) and (11) as shown in Fig. 22, with a parameter as the vertical borehole spacing d_0 . Here, assuming that the shotcreted zone permeability K_3 is equal to the relaxed zone permeability K_2 , the horizontal drain borehole spacing d is determined in the condition that the discharge flow rate to the cavern will become equal to the discharge flow rate into the horizontal drain borehole. Thus, it is possible to decrease the high groundwater pressure at the behind shotcreted zone due to $K_2 \gg K_3$ under the same condition as $K_2 = K_3$. From Fig. 22, the horizontal drain borehole spacing d which becomes the same condition as $K_2 = K_3$ is determined. The obtained results are summarized in table 3.

Namely, the vertical drain boreholes are arranged upward from the drain tunnel about 20 m away from the cavern at spacing of $d_0 = 5 \sim 10$ m. And the horizontal drain boreholes are arranged in the base of cavern wall at spacing of $d = 10$ m (length ; 10 m) with respective borehole diameter being $2r_0 = 2r = 50$ mm. Consequently, it will be possible to prevent the growth of groundwater discharge into the cavern and also to prevent the apply of high groundwater head at the behind shotcreted zone. Because the groundwater head h_2 becomes almost the cavern bottom.

3.4 Examination Using The Groundwater Discharge Into The Drain Boreholes And Convergence Of The Cavern Width

The validity of the drain system was examined as described below, on the basis of measured results concerning the discharge flow rate into the drain boreholes ($d_0 = 12$ m, horizontal drain boreholes : none) and convergence of cavern width at excavating

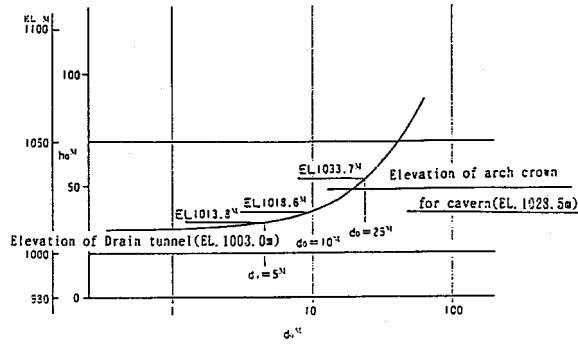


Fig. 20 $d_o - h_o$ Curve.

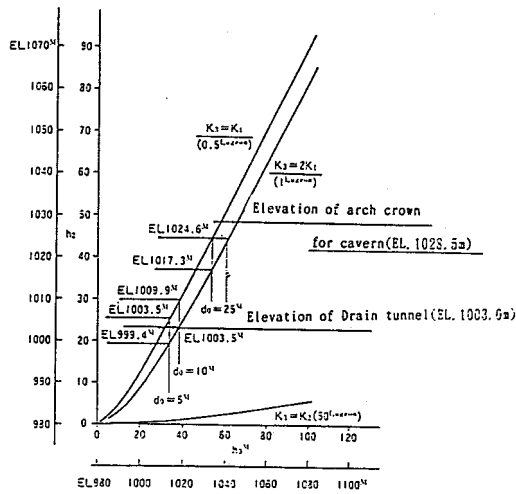


Fig. 21 $h_o - h_2$ Curve.

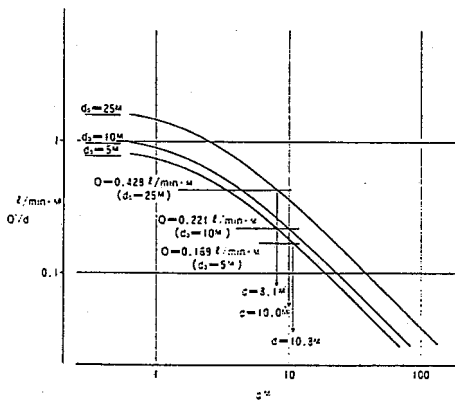


Fig. 22 $d - Q/d$ Curve.

Table 3 Results of the examination.

vertical drain boreholes		horizontal drain boreholes		
d m	h EL m	d m	h EL m	Q /min
5.0	1,013.8	10.8	980.9	1.38
10.0	1,018.6	10.0	981.1	2.21
25.0	1,033.7	8.1	982.0	3.47

Where,

d : Spacing of vertical drain boreholes.

h : Groundwater head at the intermediate point between the vertical drain boreholes (A conversion value for elevation).

d : Spacing of horizontal drain boreholes.

h : Groundwater head at the intermediate point between the horizontal drain boreholes (A conversion value for elevation).

Q : Groundwater discharge flow rate into the horizontal drain boreholes.

period the cavern. The convergence is measured in each 5 cross-sections both horizontal and vertical as shown in Fig. 23, and the discharge flow rate is measured in the section of about 100 m on the side of F and G cross-sections as shown in the same figure. These side of F and G cross-sections have inferior bedrock as compared with the side of C, D and E cross-sections, and the water discharge is found concentrated in these sections.

A correlation between the discharge flow rate and the convergence is shown in Figs. 24-1~7, and are summarized in Table 4. In this case, as to the convergence, values of just after excavating the cavern are excluded, therefore displacements due to blasting, etc. for excavation are not included. According to Table 4, the coefficient of correlation between the discharge flow rate and the convergence is $R = 0.350 \sim 0.618$ (Average ; 0.512) in the side of F and G cross-sections, also, is $R = 0.042 \sim 0.369$ (Average ; 0.216) in the side of C, D and E cross-sections. This coefficient of correlation in the side of F and G cross-sections larger as its in the side of C, D and E cross-sections. Moreover, the significance of the coefficient of correlation in the side of F and G cross-sections are higher level as its the side of C and D cross-sections, indicate that the effect of groundwater is also one of the primary factors of displacement in the side of F and G cross-sections.

According to Fig. 24, the convergence when the discharge flow rate is 80 ~ 100 ℓ /min or less varies widely with 0.25 mm converted per day, thus it is not find a significance displacement due to groundwater. However, when the discharge flow rate exceeds this flow rate, the convergence increases as the discharge flow rate becomes increases. Namely, the function of drain boreholes is acting effectively until the total discharge flow rate reaches 80 ~ 100 ℓ /min. However, when groundwater pressure around the cavern becomes high pressure which is enough to exceed 80 ~ 100 ℓ /min, the drain effect declines, and the convergence increases as the groundwater pressure becomes increases.

Then, the correlation between the discharge flow rate into the drain borehole and the groundwater head is examined on the

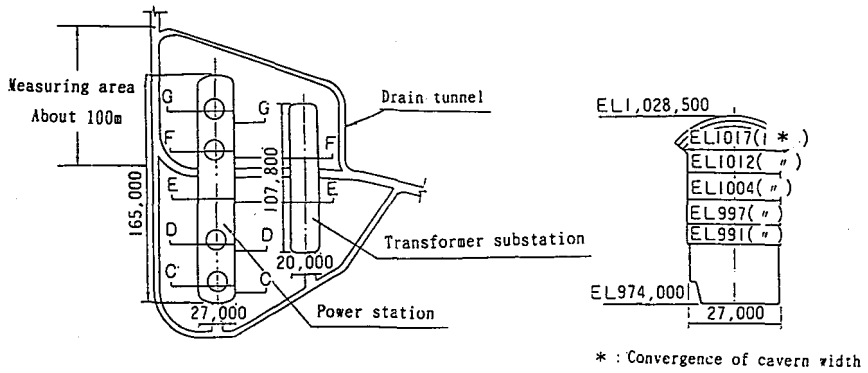


Fig.23 Measuring area of the ground water discharge and convergence of cavern width.

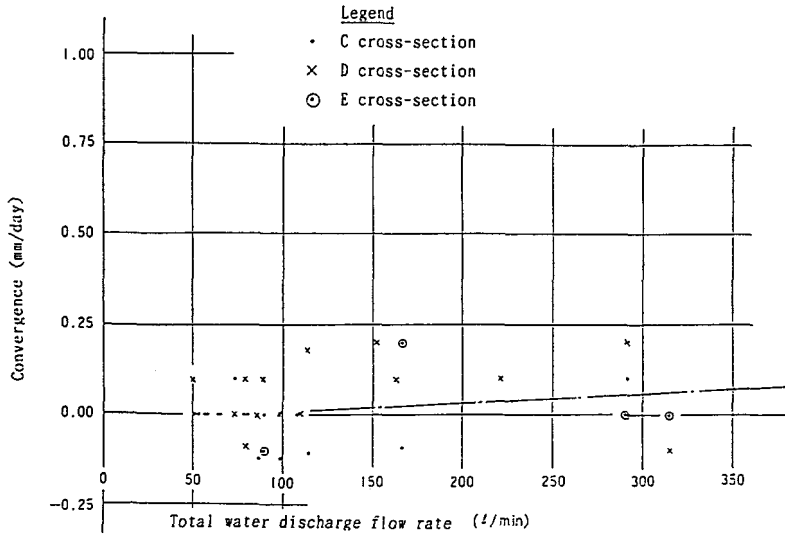


Fig.24-1 Relationship between the ground water discharge and convergence of cavern width(EL 1,017 m).

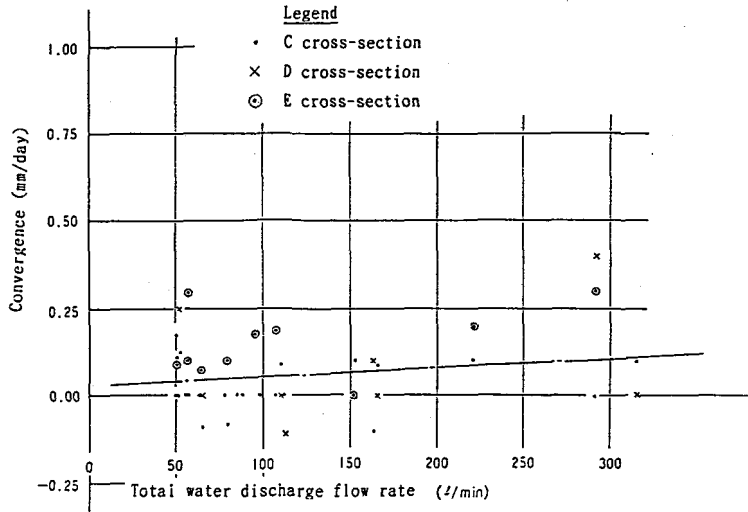


Fig.24-4 Relationship between the ground water discharge and convergence of cavern width(EL 997 m).

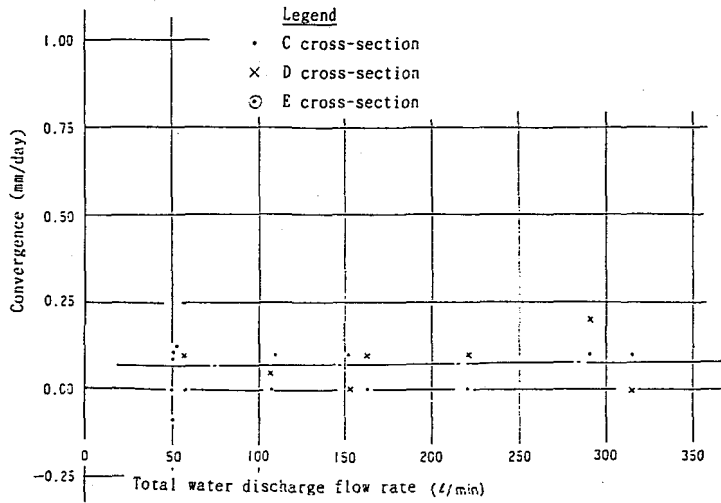


Fig.24-5 Relationship between the ground water discharge and convergence of cavern width(EL 991 m).

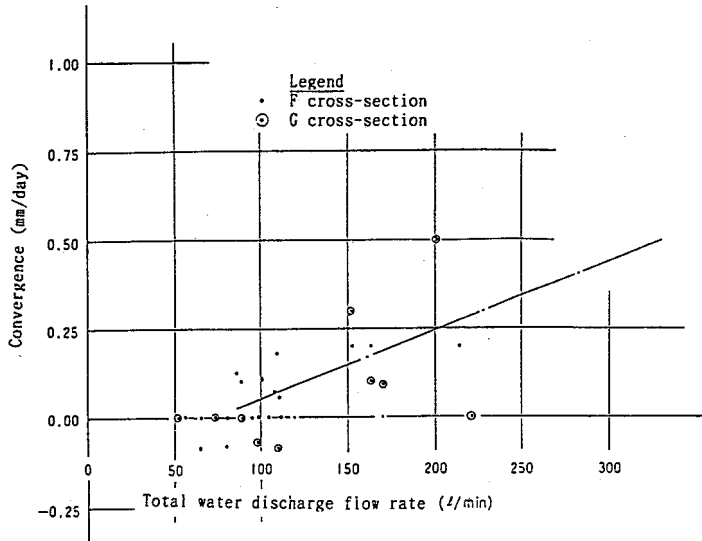


Fig.24-6 Relationship between the ground water discharge and convergence of cavern width(EL 1,017 m).

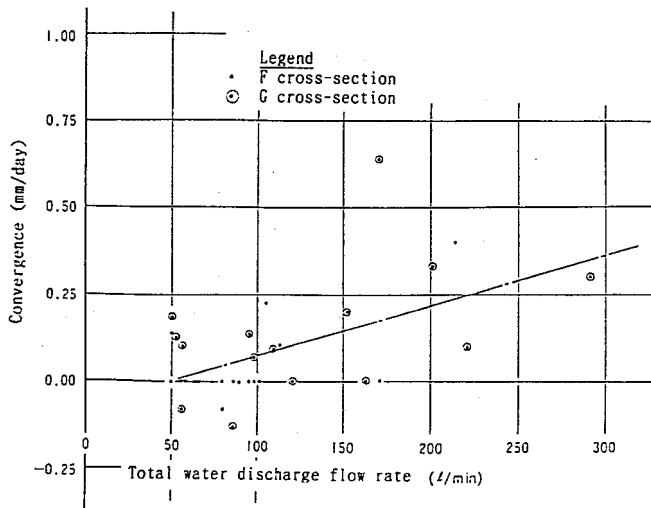


Fig.24-7 Relationship between the ground water discharge and convergence of cavern width(EL 1,012 m).

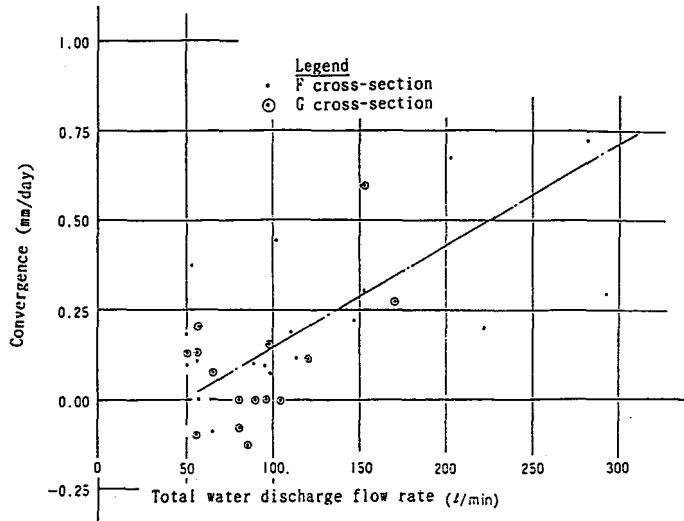


Fig.24-8 Relationship between the ground water discharge and convergence of cavern width(EL 1,004 m).

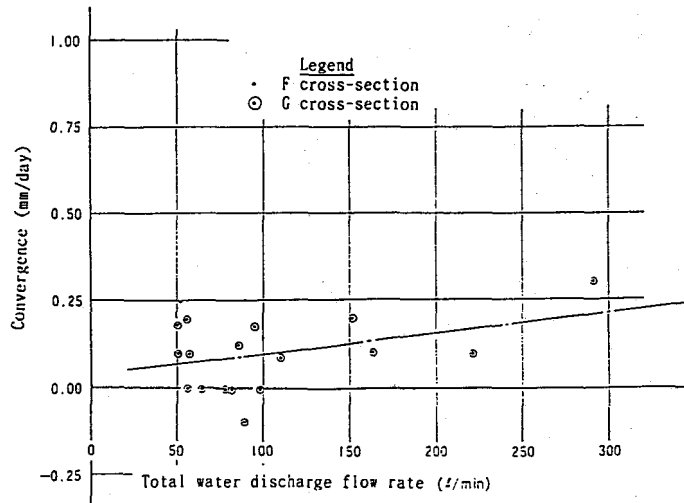


Fig.24-9 Relationship between the ground water discharge and convergence of cavern width(EL 997 m)

Table 4-1 Relationship between the ground water discharge and convergence of cavern width (C,D and E cross-section)

EL. m	Coefficient of correlation	Level of Significance %
1,017	0.246	95.0
1,012	0.369	99.1
1,004	0.232	95.0
997	0.192	70.0
991	0.042	10.0

Table 4-2 Relationship between the ground water discharge and convergence of cavern width (F and G cross-section).

EL. m	Coefficient of correlation	Level of Significance %
1,017	0.618	99.9
1,012	0.567	99.9
1,004	0.512	99.9
997	0.350	70.0

basis of the theoretical studies described in the preceding chapter.

Here, the discharge flow rate q_0 obtained in Chapter 2-2 is the discharge flow rate per unit length of one borehole, hence the discharge flow rate Q cannot be identified immediately.

Using the Dupuit-Forchheimer's hypothesis, therefore, the discharge flow rate Q into the drain borehole is obtained by the following equation :

$$Q_0 = \frac{\pi K(H_0^2 - h_{w0}^2)}{\ln \frac{\sinh \frac{2\pi}{d_0} l_0}{\sinh \frac{\pi}{d_0} r_0}} \dots \dots \dots (12)$$

When the discharge flow rate Q is 80 ~ 100 ℓ/min, the groundwater head h_{00} at an intermediate point between drain boreholes is calculated by equations (7) and (12), with $K = 0.5$ Lugeon, $l_0 = 190$ m, $2r_0 = 50$ mm, $h_{w0} = 30$ m which are the constants used in the preceding studies, on the assumption that the vertical drain borehole spacing d_0 is 12.0 m at the excavated time of the cavern. As a result, $h_0 = 44.4 \sim 46.2$ m (EL 1024.4 ~ 1026.2 m) is obtained. This elevation is located between the arch abutment(EL 1017 m) and the arch crown of the cavern(EL 1028.5 m).

Meanwhile, the maximum discharge flow rate $Q = 315$ ℓ/min can be obtained from Fig. 24. The natural groundwater head at this case is obtained from equation (12), then $H_0 = 469.1$ m. The maximum natural groundwater head is assumed to be 1.5 times, $H = 700$ m(EL 1680 m), for safety, to calculate the groundwater head h at an intermediate point between drain boreholes. Consequently, the groundwater head $h_0 = 62.3$ m(EL 1042.3 m) and the discharge flow rate $Q = 370$ ℓ/min can be calculated. This natural groundwater head $H_0 = 700$ m is equivalent to a static pressure when the whole bedrock is saturated by the groundwater.

Then, the drain borehole spacing require to decrease the groundwater head at an intermediate point between drain boreholes to $h_0 = 44.4 \sim 46.2$ m is obtained. In Fig. 25, the

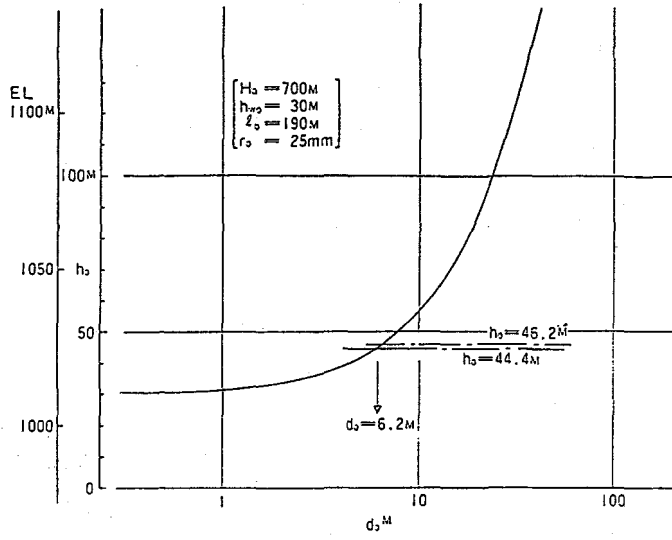


Fig.25 $d_o - h_o$ curve.

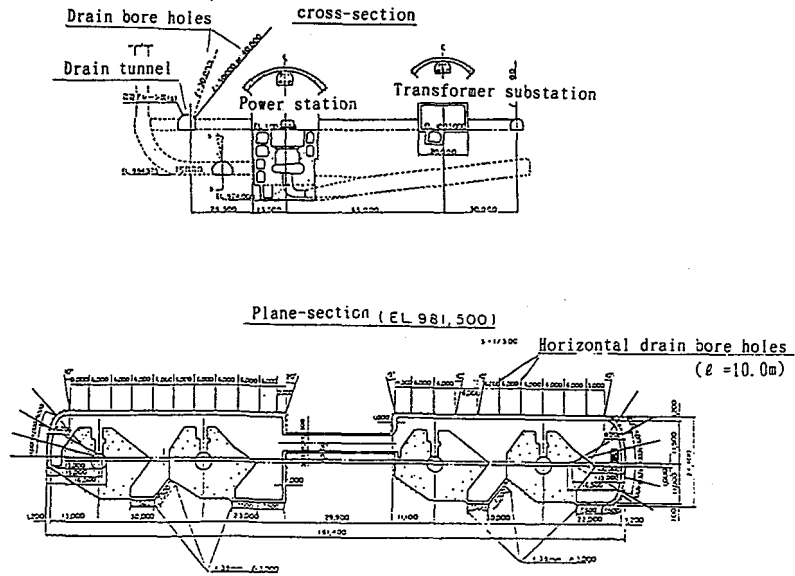


Fig.26 Arrangement of drain bore holes.

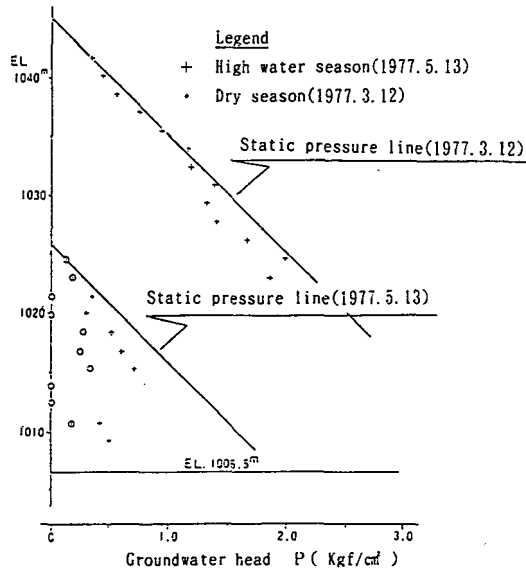


Fig.27 Groundwater head at the vertical drain bore holes.

relationship between the groundwater h_0 and the borehole spacing d_0 is obtained, by which the borehole spacing $d_0 = 6.2$ m is obtained.

The practical arrangement drawing of the vertical drain boreholes and horizontal drain boreholes are shown in Fig. 26. The vertical drain boreholes are arranged at spacing of $d_0 = 6$ m and a lengths of $L = 30 \sim 50$ m in the drain tunnel located on the mountains side of about 20 m from the cavern, mainly around the F and G cross-sections side in which the groundwater discharge is concentrated, while the horizontal drain boreholes are arranged at spacing of $d_0 = 6$ m and a lengths of $L = 10$ m in the base of cavern wall. An example of measured on the groundwater pressure at the 1.5 m section in the vertical drain boreholes are shown in Fig. 27. This figure indicates that the groundwater pressure decreases almost below EL 1024 m even during a high water season.

It can, therefore, be judged that the drain system carried out at this cavern has achieved an objective for decreasing the groundwater pressure around the cavern to a limited groundwater pressure at an intermediate point between drain boreholes, which no causes the convergence as mentioned above, and that the drain effect is acting effectively.

4. CONCLUSION

The behavior of groundwater is integral with meteorology, topography, geologic factors, etc. Particularly, its behavior in the bedrock is greatly governed by complicated geologic factors. For consideration a groundwater flow in the bedrock, it is important to identify its behavior as the whole of the groundwater flow system taking into account these factors.

In this report, the method (drain systems) for decreasing the groundwater pressure around the cavern are theoretically studied and are examined the cavern for the Shin Takasegawa Power Station constructed by Tokyo Electric Power Co., Inc. as a model. As a result, the effectiveness of this study was proved, and indicating that the drain system around the cavern for the Shin Takasegawa Power Station is acting effectively.

These are two important points in examining the drain system.

One is the evaluation of the natural groundwater head, and another is a criteria for the decreasing of groundwater head. The former is exactly a problem relating to the behavior of the groundwater in the bedrock and involves complicated problems that must be solved in the future. However, according to this study, it can be considered that one standard is to use a static pressure under which the whole bedrock becomes a saturated condition, as natural groundwater head and to provide an elevation of arch abutment for cavern on the vertical drain borehole line in the area about 20 m away from the cavern, as a criteria for the decreasing of groundwater head.

For the future, especially in considering rational drain systems, it will be very important to examine these problems more substantiatively.

In conclusion, the author would like to acknowledge the cooperation of Mr. Ikeda, Director (then), No. 2 Construction Site, Takasegawa Hydraulic Power Construction Office, Tokyo Electric Power co., Inc. and other persons concerned.

REFERENCES

- (1) H. Takahashi: Journal of the Japan Society of Engineering Geology, 6-1 (1964), 25-52.
- (2) T. Kasama and M. Tsurumaki: Journal of the Japan Society of Engineering Geology, Vol. 12-1 (1971), 16-28.
- (3) K. Miki and H. Yoshizawa: Transactions of the Japan society of Civil Engineers, 282 (1979), 31-43.
- (4) Y. Seki: Journal of the Japan Society of Engineering Geology, 22-1 (1981), 132-144.
- (5) T. Adachi and T. Tamura: Transactions of the Japan society of civil Engineers, 280 (1978), 87-98.
- (6) H. Komada, N. Nakagawa, Y. Kitahara and M. Hayashi: CREPI Report (1979) NO. 378028.
- (7) N. Tanaka and S. Aki: CREPI Report (1979), NO. 379006
- (8) K. Sato ; The Japanese Society of Soil Mechanics and Foundation Engineering, 29-12 (1981).
- (9) I. Motojima: CREPI Report (1979), NO. 379009.
- (10) K. Kashuya and K. Saito: CREPI Report (1971), NO. 376528.
- (11) Y. Hori and K. Miyakoshi: CREPI Report (1977), NO. 376528.